Asymmetric problem of a row of revolutional ellipsoidal cavities using singular integral equations

Nao-Aki Noda [a,*], Nozomu Ogasawara [a], Tadatoshi Matsuo [b]

[a] *Department of Mechanical Engineering, Kyusyu Institute of Technology, 1-1 Sensui-cho Tobata, Kitakyusyu 804-8550, Japan*
[b] *Department of Mechanical Engineering, Fukushima National College of Technology, Iwaki 970-8034, Japan*

Abstract

This paper deals with numerical solution of singular integral equations of the body force method in an interaction problem of revolutional ellipsoidal cavities under asymmetric uniaxial tension. The problem is solved on the superposition of two auxiliary loads; (i) biaxial tension and (ii) plane state of pure shear. These problems are formulated as a system of singular integral equations with Cauchy-type singularities, where the unknowns are densities of body forces distributed in the r, θ, z directions. In order to satisfy the boundary conditions along the ellipsoidal boundaries, eight kinds of fundamental density functions proposed in our previous papers are applied. In the analysis, the number, shape, and spacing of cavities are varied systematically; then the magnitude and position of the maximum stress are examined. For any fixed shape and size of cavities, the maximum stress is shown to be linear with the reciprocal of squared number of cavities. The present method is found to yield rapidly converging numerical results for various geometrical conditions of cavities.
© 2003 Elsevier Science Ltd. All rights reserved.

Keywords: Elasticity; Stress concentration; Body force method; Ellipsoidal cavity; Singular integral equation; Tension

1. Introduction

To evaluate the effect of defects on the strength of structures, it is important to analyze the stress concentration problems of ellipsoidal cavities in infinite bodies under tension. In previous research, two spherical cavities were treated by Sternberg and Sadowsky (1952), Eubanks (1965) and Miyamoto (1957); two rigid inclusions were analyzed by Hill (1966), Shelly and Yu (1966) and Goree and Wilson (1967). In addition, an infinite row of spherical cavities were solved by Atsumi (1960); an infinite row of ellipsoidal cavities were treated by Nisitani (1963). Recently, the authors have also considered ellipsoidal cavities using singular integral equations of the body force method (Noda and Matsuo, 1995b, 1996). This method can be applied to the analysis for various shapes and spacing of cavities. However, all of those studies mentioned

---

Nomenclature

a	major radius of revolutional ellipsoidal cavity
b	minor radius of revolutional ellipsoidal cavity
d	spacing of cavities
(x, y, z), (r, θ, z)	rectangular and cylindrical coordinates
(ξ, η, ζ), (ρ, ϕ, ζ)	rectangular and cylindrical coordinates where body forces are distributed
ψ_i	angle specifying the point (r, θ, z)
ψ_{i0}	angle between the r-axis and normal direction of ellipsoid in the plane $\theta = 0$
α_k	angle specifying the point (ρ, ϕ, ζ)
$\sigma_r^{F_r}$	stress component due to a single ring force
$K_{nn}^{F_r}$	singular kernel, which means, stress component due to two ring forces F_r acting symmetrically to the plane $z = 0$
F_r	ring force distributed in the r-direction whose magnitude is proportional to $\cos 2\phi$
F_θ	ring force distributed in the q-direction whose magnitude is proportional to $\sin 2\phi$
F_z	ring force distributed in the z-direction whose magnitude is proportional to $\cos 2\phi$
N	number of cavities
M	number of collocation points for each cavity

above are concerned with axisymmetric problems. Concerning axisymmetric cavities under asymmetric loads, only two and three spherical cavities in an infinite body were analyzed by Tsuchida et al. (1976, 1978).

This paper deals with a row of revolutional ellipsoidal cavities in an infinite body under asymmetric uniaxial load using singular integral equations of the body force method. Then, the interaction effects are discussed with varying the shape and spacing of ellipsoidal cavities. The present method of analysis yields the smooth variation of stress distribution along the boundaries.

2. Analysis method

Consider an infinite body under asymmetric uniaxial tension having ellipsoidal cavities as shown in Fig. 1(c). This problem is composed of the superposition of Problems A and B as shown in Fig. 1. Rectangular and cylindrical coordinates (x, y, z) and (r, θ, z) are defined in Fig. 1. Here, (ξ, η, ζ) and (ρ, ϕ, ζ) are rectangular and cylindrical coordinates that specify the points where body forces are distributed. The problem A can be analyzed by applying the method described in the preceding paper (Noda and Matsuo, 1996). In this paper, therefore, the solution of the problem B will be mainly explained. The body force method is used to formulate the problem as a system of singular integral equations. Then, the fundamental solutions are stress fields $K_{nn}^{F_r} + K_{nn}^{F_\theta}$, $K_{nn}^{F_z}$, $K_{nt}^{F_r} + K_{nt}^{F_\theta}$, $K_{nt}^{F_z}$ at an arbitrary point $[r = a \cos \psi_i,\ z = d + 2d(i-1) + b \sin \psi_i,\ i = 1, 2, \ldots, N/2]$ when two ring forces acting symmetrically to the plane $z = 0$ $[\rho = a \cos \alpha_k,\ \zeta = \pm\{d + 2d(k-1) + b \sin \alpha_k\},\ k = 1, 2, \ldots, N/2]$. The problem B is symmetric with respect to $z = 0$. Therefore if we use the fundamental solution due to two ring forces instead of a single ring force, we can consider the boundary condition only on $z \geqslant 0$. Here, each ring force has the magnitude proportional to $\cos 2\phi$ or $\sin 2\phi$ along the circumference. The integral equations are expressed by Eq. (1), where the unknowns are densities of body force distributed along the prospective boundaries. $\rho_r^*(\alpha_k)$, $\rho_\theta^*(\alpha_k)$, $\rho_z^*(\alpha_k)$. Here, equally spaced equal N ellipsoidal cavities shown in Fig. 2, where N is an even number, are assumed
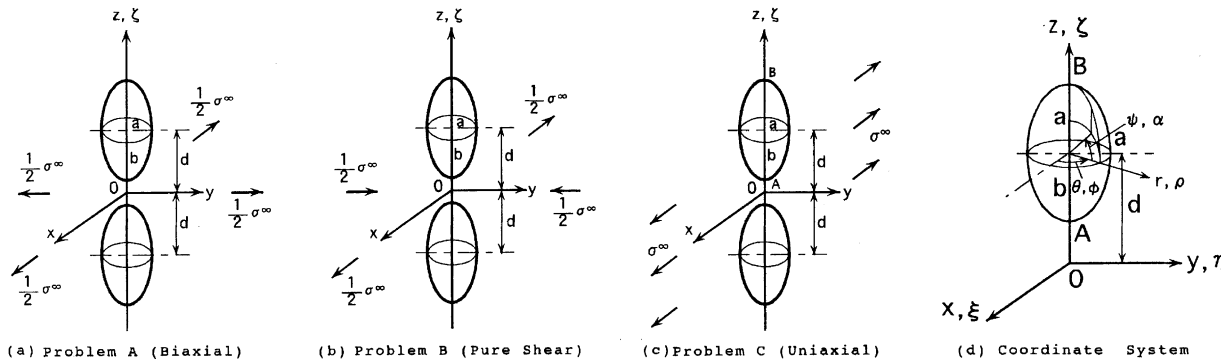
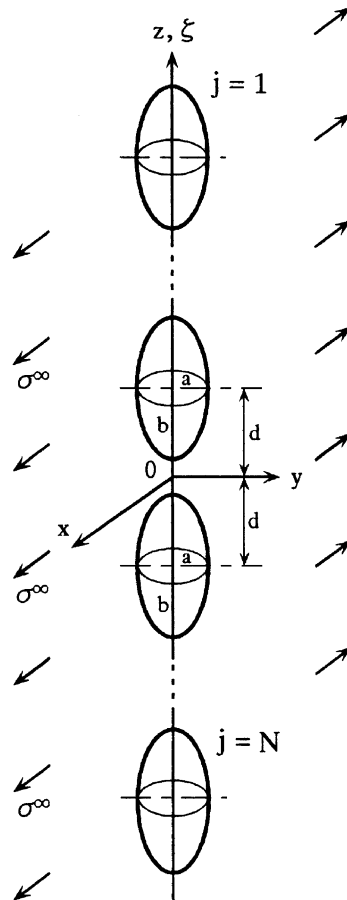Fig. 1. Problem and coordinate system for two ellipsoidal cavities.

Fig. 2. A row of revolutional ellipsoidal cavities in an infinite body.

to explain the solution. The method also can be applied to the case when N is an odd number. The notation α_k is the angle that specifies the points where body forces are distributed.

$$\left(-\frac{1}{2}\right)\{\rho_r^*(\psi_i)\cos\psi_{i0} + \rho_z^*(\psi_i)\sin\psi_{i0}\} + \sum_{k=1}^{N/2}\int_{-\pi/2}^{\pi/2}K_{nn}^{F_r}(\alpha_k,\psi_i)\rho_r^*(\alpha_k)\,\mathrm{d}s$$

$$+ \sum_{k=1}^{N/2}\int_{-\pi/2}^{\pi/2}K_{nn}^{F_\theta}(\alpha_k,\psi_i)\rho_\theta^*(\alpha_k)\,\mathrm{d}s + \sum_{k=1}^{N/2}\int_{-\pi/2}^{\pi/2}K_{nn}^{F_z}(\alpha_k,\psi_i)\rho_z^*(\alpha_k)\,\mathrm{d}s$$

$$= -\sigma_r^\infty\cos^2\psi_{i0}\cos 2\theta$$

$$\left(-\frac{1}{2}\right)\{-\rho_r^*(\psi_i)\sin\psi_{i0} + \rho_z^*(\psi_i)\cos\psi_{i0}\} + \sum_{k=1}^{N/2}\int_{-\pi/2}^{\pi/2}K_{nt}^{F_r}(\alpha_k,\psi_i)\rho_r^*(\alpha_k)\,\mathrm{d}s$$

$$+ \sum_{k=1}^{N/2}\int_{-\pi/2}^{\pi/2}K_{nt}^{F_\theta}(\alpha_k,\psi_i)\rho_\theta^*(\alpha_k)\,\mathrm{d}s + \sum_{k=1}^{N/2}\int_{-\pi/2}^{\pi/2}K_{nt}^{F_z}(\alpha_k,\psi_i)\rho_z^*(\alpha_k)\,\mathrm{d}s$$

$$= -\sigma_r^\infty\sin\psi_{i0}\cos\psi_{i0}\cos 2\theta \quad i = 1, 2, \ldots, N/2$$

(1)

where

$$\left.\begin{array}{l}-\mathrm{d}\rho = a\sin\alpha_k\,\mathrm{d}\alpha_k, \quad \mathrm{d}\zeta = b\cos\alpha_k\,\mathrm{d}\alpha_k \\ \mathrm{d}s = \sqrt{a^2\sin^2\alpha_k + b^2\cos^2\alpha_k}\,\mathrm{d}\alpha_k\end{array}\right\}$$

(2)

In Eq. (1), the singular kernels $(K_{nn}^{F_r} + K_{nn}^{F_\theta}, K_{nn}^{F_z}, K_{nt}^{F_r} + K_{nt}^{F_\theta}, K_{nt}^{F_z})$ denote normal stress σ_n and shear stress τ_{nt} appearing at the prospective boundary for cavities induced by two ring forces acting in the r, θ, z directions along two circumferences. Here ψ_{i0} is the angle between the r-axis and the normal direction of ellipsoid at (r, z) in the plane $\theta = 0$. The notation $\sigma_r^\infty\cos 2\theta$ stands for the stress field of pure shear at infinity $r \to \infty$. Eq. (1) enforce boundary conditions at the imaginary boundary; that is, $\sigma_n = 0$ and $\tau_{nt} = 0$. The first terms of Eq. (1) represent the stress due to the body force distributed on "the minus boundary" (Nisitani, 1967). "The minus boundary" (− boundary in Nisitani's paper) means the imaginary boundary composed of the internal points that are infinitesimally apart from the initial boundary. The second and third terms of Eq. (1) include the singular terms having the singularity of the form $1/\sin\{(\psi_I - \alpha_k)/2\}$. In this case $\psi_i = \alpha_k$, $i = k$, the integration should be interpreted in Cauchy principal value sense. The unknown functions in eqns $\rho_r^*(\alpha_k)$, $\rho_\theta^*(\alpha_k)$, $\rho_z^*(\alpha_k)$ are expressed by the following equations.

$$\left.\begin{array}{l}\rho_r^*(\alpha_k)\cos 2\phi = \dfrac{\mathrm{d}F_r}{\rho\,\mathrm{d}\phi\,\mathrm{d}s} \\[2mm] \rho_\theta^*(\alpha_k)\sin 2\phi = \dfrac{\mathrm{d}F_\theta}{\rho\,\mathrm{d}\phi\,\mathrm{d}s} \\[2mm] \rho_z^*(\alpha_k)\cos 2\phi = \dfrac{-\mathrm{d}F_z}{\rho\,\mathrm{d}\phi\,\mathrm{d}s}\end{array}\right\}$$

(3)

where $\mathrm{d}F_r$, $\mathrm{d}F_\theta$, $\mathrm{d}F_z$ are the components of the resultant of the body force in the r, θ, z directions acting on the infinitesimal area $\rho\,\mathrm{d}\phi\,\mathrm{d}s$, respectively.

In a similar way of the preceding paper (Noda and Matsuo, 1996), new fundamental density functions of the body force in the r, θ, z directions $w_r(\alpha_k)$, $w_\theta(\alpha_k)$, $w_z(\alpha_k)$ are defined by the following equations (Noda and Matsuo, 1993, 1995a,b).

$$
\begin{aligned}
&w_{r1}(\alpha_k) = n_r(\alpha_k)/\cos\alpha_k && w_{r2}(\alpha_k) = n_r(\alpha_k)\tan\alpha_k \\
&w_{r3}(\alpha_k) = n_r(\alpha_k) && w_{r4}(\alpha_k) = n_r(\alpha_k)\sin\alpha_k \\
&w_{\theta1}(\alpha_k) = n_r(\alpha_k)/\cos\alpha_k && w_{\theta2}(\alpha_k) = n_r(\alpha_k)\tan\alpha_k \\
&w_{\theta3}(\alpha_k) = n_r(\alpha_k) && w_{\theta4}(\alpha_k) = n_r(\alpha_k)\sin\alpha_k \\
&w_{z1}(\alpha_k) = n_z(\alpha_k)/\cos\alpha_k && w_{z2}(\alpha_k) = n_z(\alpha_k) \\
&w_{z3}(\alpha_k) = n_z(\alpha_k)\cot\alpha_k && w_{z4}(\alpha_k) = n_z(\alpha_k)\cos\alpha_k
\end{aligned} \tag{4}
$$

Here, $n_r(\alpha_k)$, $n_z(\alpha_k)$ are the r, z components $(\cos\psi_{i0}, \sin\psi_{i0})$ of the normal unit vector, respectively, at the point (r, z). They are expressed by the following equations.

$$
n_r(\alpha_k) = \frac{b\cos\alpha_k}{\sqrt{a^2\sin^2\alpha_k + b^2\cos^2\alpha_k}}, \quad n_z(\alpha_k) = \frac{a\sin\alpha_k}{\sqrt{a^2\sin^2\alpha_k + b^2\cos^2\alpha_k}} \tag{5}
$$

In the present analysis, the unknown functions of the body force densities for ellipsoidal cavities $\rho_r^*(\alpha_k)$, $\rho_\theta^*(\alpha_k)$, $\rho_z^*(\alpha_k)$ can be expressed as a linear combination of the fundamental density functions defined by Eq. (4) and the weight functions $\rho_{r3}(\alpha_k)$, $\rho_{r4}(\alpha_k)$, $\rho_{\theta3}(\alpha_k)$, $\rho_{\theta4}(\alpha_k)$, $\rho_{z1}(\alpha_k)$, $\rho_{z2}(\alpha_k)$ as shown in the following Eq. (6). These weight functions are symmetric with respect to the axis $\alpha_k = 90°$, namely, the z-axis.

$$
\left.
\begin{aligned}
\rho_r^*(\alpha_k) &= \rho_{r3}(\alpha_k)w_{r3}(\alpha_k) + \rho_{r4}(\alpha_k)w_{r4}(\alpha_k) \\
\rho_\theta^*(\alpha_k) &= \rho_{\theta3}(\alpha_k)w_{\theta3}(\alpha_k) + \rho_{\theta4}(\alpha_k)w_{\theta4}(\alpha_k) \\
\rho_z^*(\alpha_k) &= \rho_{z2}(\alpha_k)w_{z2}(\alpha_k) + \rho_{z1}(\alpha_k)w_{z1}(\alpha_k)
\end{aligned}
\right\} \tag{6}
$$

Using the expressions in Eq. (6), the singular integral Eq. (1) is reduced to following Eq. (7).

$$
\begin{aligned}
&\left(-\frac{1}{2}\right)\left[\{\rho_{r3}(\psi_i) + \rho_{r4}(\psi_i)\sin\psi_i\}\cos^2\psi_{i0} + \{\rho_{z2}(\psi_i) + \rho_{z1}(\psi_i)/\sin\psi_i\}\sin^2\psi_{i0}\right] \\
&\quad + \sum_{k=1}^{N/2}\int_{-\pi/2}^{\pi/2} K_{nn}^{F_r}(\alpha_k, \psi_i)\{\rho_{r3}(\alpha_k) + \rho_{r4}(\alpha_k)\sin\alpha_k\}b\cos\alpha_k\,\mathrm{d}\alpha_k \\
&\quad + \sum_{k=1}^{N/2}\int_{-\pi/2}^{\pi/2} K_{nn}^{F_\theta}(\alpha_k, \psi_i)\{\rho_{\theta3}(\alpha_k) + \rho_{\theta4}(\alpha_k)\sin\alpha_k\}b\cos\alpha_k\,\mathrm{d}\alpha_k \\
&\quad + \sum_{k=1}^{N/2}\int_{-\pi/2}^{\pi/2} K_{nn}^{F_z}(\alpha_k, \psi_i)\{\rho_{z2}(\alpha_k) + \rho_{z1}(\alpha_k)/\sin\alpha_k\}a\sin\alpha_k\,\mathrm{d}\alpha_k = -\sigma_r^\infty\cos^2\psi_{i0}\cos2\theta \\[4pt]
&\left(-\frac{1}{2}\right)\left[-\{\rho_{r3}(\psi_i) + \rho_{r4}(\psi_i)\sin\psi_i\} + \{\rho_{z2}(\psi_i) + \rho_{z1}(\psi_i)/\sin\psi_i\}\right]\sin\psi_{i0}\cos\psi_{i0} \\
&\quad + \sum_{k=1}^{N/2}\int_{-\pi/2}^{\pi/2} K_{nt}^{F_r}(\alpha_k, \psi_i)\{\rho_{r3}(\alpha_k) + \rho_{r4}(\alpha_k)\sin\alpha_k\}b\cos\alpha_k\,\mathrm{d}\alpha_k \\
&\quad + \sum_{k=1}^{N/2}\int_{-\pi/2}^{\pi/2} K_{nt}^{F_\theta}(\alpha_k, \psi_i)\{\rho_{\theta3}(\alpha_k) + \rho_{\theta4}(\alpha_k)\sin\alpha_k\}b\cos\alpha_k\,\mathrm{d}\alpha_k \\
&\quad + \sum_{k=1}^{N/2}\int_{-\pi/2}^{\pi/2} K_{nt}^{F_z}(\alpha_k, \psi_i)\{\rho_{z2}(\alpha_k) + \rho_{z1}(\alpha_k)/\sin\alpha_k\}a\sin\alpha_k\,\mathrm{d}\alpha_k \\
&= -\sigma_r^\infty\sin\psi_{i0}\cos\psi_{i0}\cos2\theta \quad i = 1, 2, \ldots, N/2
\end{aligned} \tag{7}
$$

In the analysis of plane state of pure shear as shown in Problem B of Fig. 1 it should be noted that the magnitude of two types of body force densities ρ_r and ρ_θ are always identical, that is, $\rho_r^*(\alpha_k) = \rho_\theta^*(\alpha_k)$. In the analysis of pure shear, therefore, the number of unknown is $2M$, where M is the number of collocation points. On the other hand, in the analysis of an axisymmetric body under bending, the number of unknown

is $3M$, instead of $2M$ (Murakami et al., 1986a,b) although both of those are similar problems of an axisymmetric body under the asymmetric loads.

In the present analysis, polynomials have been applied to approximate the unknown functions as continuous functions. Now, from the symmetry to the axis $\alpha_k = 90°$ of the problem, the following expression can be applied.

$$\begin{cases} \rho_{r3}(\alpha_k) = \sum_{n=1}^{M/2} a_{kn}t_n(\alpha_k) \\ \rho_{r4}(\alpha_k) = \sum_{n=1}^{M/2} b_{kn}t_n(\alpha_k) \end{cases} \begin{cases} \rho_{\theta3}(\alpha_k) = \sum_{n=1}^{M/2} c_{kn}t_n(\alpha_k) \\ \rho_{\theta4}(\alpha_k) = \sum_{n=1}^{M/2} d_{kn}t_n(\alpha_k) \end{cases} \begin{cases} \rho_{z2}(\alpha_k) = \sum_{n=1}^{M/2} e_{kn}t_n(\alpha_k) \\ \rho_{z1}(\alpha_k) = \sum_{n=1}^{M/2} f_{kn}t_n(\alpha_k) \end{cases} \tag{8}$$

Using the approximation method mentioned above, we obtain the following system of linear equations for the determination of the coefficients a_{kn}, b_{kn}, c_{kn}, d_{kn}, e_{kn}, f_{kn}. The number of unknown coefficients is $3M \times N/2$. The convenient sets of the collocation points are given by Eq. (9).

$$\psi_{il} = \left(\frac{\pi}{M}\right)(l - 0.5) - \frac{\pi}{2}, \quad i = 1, \ldots, N/2, \ l = 1, 2, \ldots, M \tag{9}$$

$$\begin{aligned} \sum_{k=1}^{N/2}\sum_{n=1}^{M/2}(a_{kn}A_{kn} + b_{kn}B_{kn} + c_{kn}C_{kn} + d_{kn}D_{kn} + e_{kn}E_{kn} + f_{kn}F_{kn}) = -\sigma_r^\infty \cos^2 \psi_{i0} \cos 2\theta \\ \sum_{k=1}^{N/2}\sum_{n=1}^{M/2}(a_{kn}G_{kn} + b_{kn}H_{kn} + c_{kn}I_{kn} + d_{kn}J_{kn} + e_{kn}K_{kn} + f_{kn}L_{kn}) = -\sigma_r^\infty \sin \psi_{i0} \cos \psi_{i0} \cos 2\theta \end{aligned} \tag{10}$$

$$A_{kn} = \left(-\frac{1}{2}\right)t_n(\psi_i)\cos^2 \psi_{i0} + \sum_{k=1}^{N/2} \int_{-\pi/2}^{\pi/2} \left\{K_{nn}^{F_r}(\alpha_k, \psi_i) + K_{nn}^{F_\theta}(\alpha_k, \psi_i)\right\}t_n(\alpha_k)b\cos\alpha_k \,\mathrm{d}\alpha_k \tag{11}$$

The stresses at an arbitrary point are represented by a linear combination of the coefficients a_{kn}, b_{kn}, c_{kn}, d_{kn}, e_{kn}, f_{kn} and the influence coefficients corresponding to $A_k \sim L_{kn}$. Using the numerical solution mentioned above we will obtain the stress concentration factors and stress distribution along the boundaries.

3. Fundamental solutions and evaluation of singular integrals

The singular kernel in Eqs. (1) and (7), for example, $K_{nn}^{F_r}$, can be expressed as follows. Here, $K_{nn}^{F_r}$ is a stress component due to two ring forces F_r acting symmetrically to the plane $z = 0$ in an infinite body. On the other hand, notations $\sigma_r^{F_r}$, $\sigma_\theta^{F_r}$, $\sigma_z^{F_r}$, $\tau_{rz}^{F_r}$, $\tau_{r\theta}^{F_r}$, $\tau_{\theta z}^{F_r}$ denote stress components due to a single ring force F_r acting in an infinite body. Namely,

$$\begin{aligned} K_{nn}^{F_r} = \sum_\zeta^2 \sigma_n^{F_r} = \sum_\zeta^2 (\sigma_r^{F_r}\cos^2\psi_i + \sigma_z^{F_r}\sin^2\psi_i + 2\tau_{rz}^{F_r}\sin\psi_i\cos\psi_i) \\ K_{nt}^{F_r} = \sum_\zeta^2 \tau_{nt}^{F_r} = \sum_\zeta^2 (\sigma_z^{F_r} - \sigma_r^{F_r})\sin\psi_i\cos\psi_i + 2\tau_{rz}^{F_r}(\cos^2\psi_i - \sin^2\psi_i) \end{aligned} \tag{12}$$

In a similar way, $K_{nn}^{F_\theta}$, $K_{nt}^{F_\theta}$, $K_{nn}^{F_z}$, $K_{nt}^{F_z}$ are defined. In Eq. (12) $\sum_\zeta^2$ means summation of stresses induced by two ring forces, which is distributing symmetrically to the plane $z = 0$ on the circumferences $z = \pm\zeta$. The problem treated in this paper is symmetric with respect to $z = 0$. Therefore if we use $K_{nn}^{F_r}$ as the meaning of stress component due to two ring forces instead of a single ring force, we can consider the boundary condition only on $z \geqslant 0$. Here, each ring force has distinct variation along the circumference, which is proportional to $\cos 2\phi$ for F_r, F_z, and $\sin 2\phi$ for F_θ. These stresses are obtained as follows by integrating the

stress fields due to a point force acting in an infinite body in a similar way of the previous papers (Murakami et al., 1986a; Nisitani and Noda, 1984). First, the stress at (r, θ, z) due to a point force in the r-direction acting at (ρ, φ, ζ) is expressed as Eq. (13).

$$
\begin{aligned}
\sigma_r^{Fr} = {} & B_r[(1 - 2v)R^{-3}[-r\cos(\varphi - \theta) + \rho\{2\cos^2(\varphi - \theta) - 1\}] \\
& - 3R^{-5}\{r\cos(\varphi - \theta) - \rho\}\{r - \rho\cos(\varphi - \theta)\}^2] \\
& B_r = \frac{F_r}{8\pi(1 - v)}, \quad R^2 = r^2 + \rho^2 - 2r\rho\cos(\varphi - \theta) + (z - \zeta)^2
\end{aligned} \tag{13}
$$

Then, the stress at (r, θ) due to a ring force with intensity $\cos 2\varphi$ acting at (ρ, ζ) is given in the following way (see Nisitani and Noda, 1984).

$$
\begin{aligned}
\sigma_r^{Fr*} = {} & \int_0^{2\pi} \sigma_r^{Fr}(\varphi - \theta)|_{Fr=1} F_r \rho \cos 2\varphi \, d\varphi = \int_0^{2\pi} \sigma_r^{Fr}(\varphi') F_r \rho \cos 2(\varphi' + \theta) \, d\varphi' \\
= {} & \int_0^{2\pi} \sigma_r^{Fr}(\varphi') F_r \rho (\cos 2\varphi' \cos 2\theta - \sin 2\varphi' \sin 2\theta) \, d\varphi' = \int_0^{2\pi} \sigma_r^{Fr}(\varphi') F_r \rho \cos 2\varphi' \, d\varphi' \cos 2\theta \\
= {} & 2B_r \Bigg[(1 - 2v)(\rho I_{3,0} + r I_{3,1} - 4\rho I_{3,2} - 4r I_{3,3} + 4\rho I_{3,4}) \frac{3}{r_m^2} \big\{ -r^2 \rho I_{5,0} + r(r^2 + 2\rho^2) I_{5,1} + \\
& - \rho^3 I_{5,2} - r(2r^2 + 3\rho^2) I_{5,3} + 2\rho(2r^2 + \rho^2) I_{5,4} - 2r\rho^2 I_{5,5} \big\} \Bigg] \cos 2\theta
\end{aligned} \tag{14}
$$

$$
\begin{aligned}
& \varphi' = \varphi - \theta, \quad I_{n,m} = \frac{1}{r_m} \int_0^\pi \frac{\cos^m \varphi'}{(e - \cos \varphi')^{n/2}} \, d\varphi', \\
& e = 1 + \frac{(r - \rho)^2 + (z - \zeta)^2}{2r\rho}, \quad r_m = \sqrt{2r\rho}
\end{aligned} \tag{15}
$$

Similar expressions of the Eqs. (13)–(15) were derived by Noguchi et al. (1987) to analyze the problem of semi-infinite body with a semi-ellipsoidal pit. As seen from the above expressions, the stresses due to three types of ring forces vary along a circumference in the form of $\cos 2\theta$ or $\sin 2\theta$. These variations are identical with the ones of σ_n and τ_{nt}, respectively, which is induced by pure shear stress at $r \to \infty$. Therefore, if the boundary conditions are satisfied at an arbitrary point along the circumference on the ellipsoidal boundary by adjusting the body forces, the boundary conditions are automatically satisfied along the whole circumference. Consequently the present method does not require the division along the circumference and the problem can be treated with high accuracy with a comparatively small number of unknowns. When the body force acts on a collocation point, the integration becomes singular. In this case the direct integration is performed for the range $\alpha_k = \psi - \varepsilon_0 \sim \psi + \varepsilon_0$. Then, the integrands can be regarded as the product of three parts: (1) the fundamental solution, (2) the fundamental density functions, and (3) the weight functions; and, all of these are expressed as power series. As an example, the stress $\sigma_r^{\rho r}$ is derived in the following way.

$$
\begin{aligned}
\sigma_r^{\rho r} = {} & \int_{-\varepsilon_0}^{\varepsilon_0} \frac{\rho}{4\pi(1 - v)r_m^3} B_r \Bigg[(1 - 2v)(\rho I_{3,0} + r I_{3,1} - 4\rho I_{3,2} - 4r I_{3,3} + 4\rho I_{3,4}) \\
& + \frac{3}{r_m^2} \big\{ -r^2 \rho I_{5,0} + r(r^2 + 2\rho^2) I_{5,1} - \rho^3 I_{5,2} - r(2r^2 + 3\rho^2) I_{5,3} + 2\rho(2r^2 + \rho^2) I_{5,4} - 2r\rho^2 I_{5,5} \big\} \Bigg] w_r^*(\alpha_k) t_n(\alpha_k) \, d\varepsilon
\end{aligned} \tag{16}
$$

Here, the following relations can be applied (Noda, 1984).

$$\rho = r\left(1 + \varepsilon\frac{a}{r_i}\sin\psi_i\cdots\right)$$

$$r_i - \rho = a\varepsilon\sin\psi_i\left(1 + \frac{1}{2}\varepsilon\cot\psi_i\cdots\right)$$

$$K_1 = I_{-1,0} = \int_0^\pi (e - \cos\varphi)^{1/2}\,\mathrm{d}\varphi = \frac{2\sqrt{2}}{k}\left\{1 + \frac{1}{2}\left(\ln\frac{4}{k'} - \frac{1}{2}\right)k'^2\cdots\right\}$$

$$K_2 = I_{1,0} = \int_0^\pi \frac{1}{(e - \cos\varphi)^{1/2}}\,\mathrm{d}\varphi = \sqrt{2}k\left\{\ln\frac{4}{k'} - \frac{1}{4}\left(\ln\frac{4}{k'} - 1\right)k'^2\cdots\right\}$$

$$k = \sqrt{\frac{2}{e+1}}, \quad k' = \frac{\varepsilon}{2r}$$

$$e = 1 + \frac{R_0^2}{2r}\varepsilon^2 + \frac{(a^2 - b^2)\sin\psi_i\cos\psi_i + (a/r)\sin\psi_i R_0^2}{2r^2}\varepsilon^3\cdots$$

$$R_0^2 = a^2\sin^2\psi_i + b^2\cos^2\psi_i$$

(17)

By substituting Eq. (17) into (16), we have

$$
\sigma_r^{\rho_r} = -\int_{-\varepsilon_0}^{\varepsilon_0} \frac{1}{4\pi(1-v)}\left[\left\{\frac{(1-2v)a\sin\psi_i}{R_0^2} + \frac{2a^3\sin^3\psi_i}{R_0^4}\right\}\bigg/\varepsilon\right.
$$
$$
+ \frac{(1-2v)a\sin\psi_i}{R_0^2}\left\{-\frac{a\sin\psi_i}{2r} + \frac{\cot\psi_i}{2} - \frac{(a^2-b^2)\sin\psi_i\cos\psi_i}{R_0^2}\right\}
$$
$$
+ \frac{2a^3\sin^3\psi_i}{R_0^4}\left\{-\frac{a\sin\psi_i}{2r} + \frac{3\cot\psi_i}{2} - \frac{2(a^2-b^2)\sin\psi_i\cos\psi_i}{R_0^2}\right\}
$$
$$
\left.+ \frac{1}{10r} + \frac{a^2\sin^2\psi_i}{2rR_0^2} - \frac{(1-2v)}{30r}\left\{161 - 45\ln\left(\frac{8r}{R_o\varepsilon}\right)\right\}\right]w_r^*(\alpha_k)t_n(\alpha_k)\,\mathrm{d}\varepsilon.
$$

(18)

Next, the fundamental density functions and the weight functions are expressed in the form of power series of ε as shown in the following equation.

$$
w_r^*(\alpha_k) = \begin{cases} w_{r3}(\alpha_k) \cong \rho_r b\cos\psi_i(1 - \varepsilon\tan\psi_i) \\ w_{r4}(\alpha_k) \cong \rho_r b\cos\psi_i(1 - \varepsilon\tan\psi_i)\sin\psi_i(1 + \varepsilon\cot\psi_i) \end{cases}
$$
$$
w_\theta^*(\alpha_k) = \begin{cases} w_{\theta3}(\alpha_k) \cong \rho_\theta b\cos\psi_i(1 - \varepsilon\tan\psi_i) \\ w_{\theta4}(\alpha_k) \cong \rho_\theta b\cos\psi_i(1 - \varepsilon\tan\psi_i)\sin\psi_i(1 + \varepsilon\cot\psi_i) \end{cases}
$$
$$
w_z^*(\alpha_k) = \begin{cases} w_{z3}(\alpha_k) \cong \rho_z a\sin\psi_i(1 - \varepsilon\cot\psi_i) \\ w_{z4}(\alpha_k) \cong \rho_z a \end{cases}
$$

(19)

$$t_n(\alpha_k) = \cos\{2(n-1)\alpha_k\} \cong \cos\{2(n-1)\psi_i\}$$

(20)

By using the Eqs. (16)–(20), the integrand is expressed as

$$f(\varepsilon) = \frac{C_{-1}}{\varepsilon} + C_0 + D_0\ln|\varepsilon| + \varepsilon(C_1 + D_1\ln|\varepsilon|) + \varepsilon^2\{C_2 + D_2(\ln|\varepsilon| - 1)\} + \cdots$$

(21)

Then, the expressions of direct integrations in the range $\alpha_k = \psi - \varepsilon_0 \sim \psi + \varepsilon_0$ can be obtained in the following way. First, for the term of $1/\varepsilon$, the integration should be interpreted as the meaning of Cauchy's

principal values. Second, the terms above ε^2 can be disregarded if we take ε small enough. Therefore, the integral of Eq. (21) is expressed as Eq. (22).

$$\sigma_r^{\rho_r} = \int_{-\varepsilon_0}^{\varepsilon_0} f(\varepsilon)\,\mathrm{d}\varepsilon \cong \int_{-\varepsilon_0}^{\varepsilon_0} (C_0 + D_0 \ln|\varepsilon|)\,\mathrm{d}\varepsilon = 2\{C_0 + D_0(\ln\varepsilon_0 - 1)\}\varepsilon_0 \tag{22}$$

4. Results and discussion for two ellipsoidal cavities

In this section, first, the results of two ellipsoidal cavities in Fig. 1 will be shown. Table 1 shows convergency of the stresses at points A ($\psi = -90°$) and B ($\psi = 90°$) with increasing the collocation number M when $a/b = 1/4$, $b/d = 2/3$, $\sigma^\infty = 1$, $v = 0.3$ in Fig. 1. The present results have shown good convergence to the fifth digit when $M = 20$. Table 2 shows the magnitude and position of the maximum stress, and the magnitude of stresses at points A ($\psi = -90°$) and B ($\psi = 90°$) for two spherical cavities when $a/b = 1.0$, $\sigma^\infty = 1$, $v = 0.3$ with $a/d = 0 \sim 0.9$ in Fig. 1. The results of Tsuchida et al. (1976) are also shown in Table 2. The present and Tsuchida's results coincide with each other to the fourth significant digit in most cases.

Fig. 3 shows stress distribution along the boundaries of the problems A, B, C in Fig. 1 when $a/b = 1/4$ with $b/d = 0.9$, and Fig. 4 shows the one when $a/b = 1/8$ with $b/d = 0.9$. Both figures also show the results of a single cavity corresponding to $b/d = 0$. Figs. 5 and 6 show stress distribution when $b/d = 0$ and $b/d = 0.9$, respectively, along the boundaries of the problem C with varying $a/b = 2.0, 1.0, 1/2, 1/4, 1/8$.

Table 1
Convergency of stress $\sigma_\theta|_{\theta=\pi/2}$ at points A and B ($N = 2$, $a/b = 1/4$, $b/d = 2/3$, $v = 0.3$)

ψ (deg)	M	Problem A	Problem B	Problem C
−90	12	2.7004	2.6736	2.6870
	16	2.7000	2.6736	2.6868
	20	2.6996	2.6736	2.6866
	24	2.6996	2.6736	2.6866
90	12	2.6476	2.6571	2.6523
	16	2.6500	2.6571	2.6536
	20	2.6484	2.6570	2.6527
	24	2.6484	2.6571	2.6527

Table 2
Stress concentration factor of two spherical cavities ($a/b = 1.0$)

a/d	$\sigma_{\theta\max}$		K_{tA}	K_{tB}
	(deg)	$K_{t\max}$		
0	−90 to 90 (−90 to 90)	2.0455 (2.045)	2.0455 (2.045)	2.0455 (2.045)
0.1	−2 (0)	2.0455 (2.046)	2.0454 (2.045)	2.0454 (2.045)
0.2	−10 (−10)	2.0462 (2.046)	2.0448 (2.045)	2.0454 (2.045)
0.3	−14 (−15)	2.0481 (2.048)	2.0427 (2.043)	2.0456 (2.046)
0.4	−17 (−20)	2.0521 (2.052)	2.0378 (2.038)	2.0464 (2.046)
0.5	−24 (−25)	2.0598 (2.060)	2.0307 (2.031)	2.0481 (2.048)
0.6	−31 (−30)	2.0742 (2.074)	2.0295 (2.029)	2.0512 (2.051)
0.7	−41	2.1022	2.0655	2.0561
0.8	−90 (−90)	2.2295 (2.230)	2.2295 (2.230)	2.0624 (2.062)
0.9	−90	2.7724	2.7724	2.0713

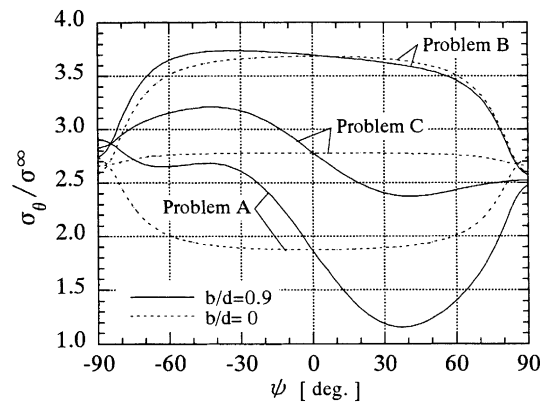Results of Tsuchida et al. (1976) in paranthesis.

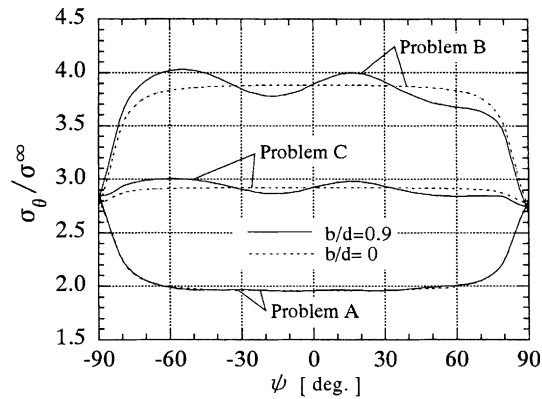Fig. 3. Distribution of stress in Fig. 1 ($N = 2$, $a/b = 1/4$, $\theta = \pi/2$).

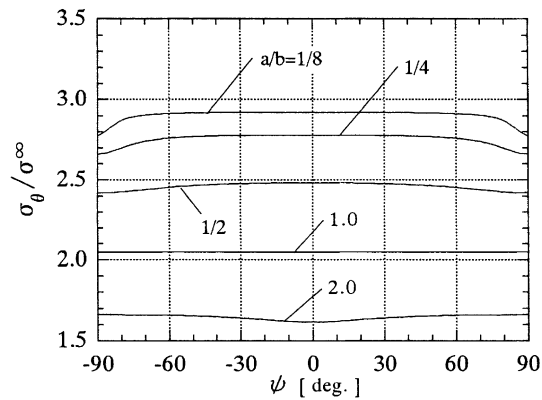Fig. 4. Distribution of stress in Fig. 1 ($N = 2$, $a/b = 1/8$, $\theta = \pi/2$).

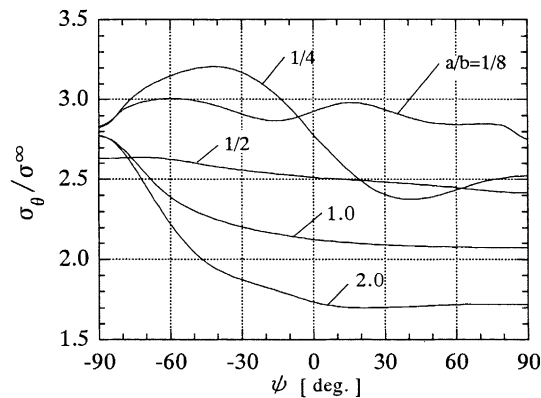Fig. 5. Distribution of stress in Fig. 1(c) ($N = 2$, $b/d = 0$, $\theta = \pi/2$).

Fig. 6. Distribution of stress in Fig. 1(c) ($N = 2$, $b/d = 0.9$, $\theta = \pi/2$).

As shown in Fig. 5, the results when $b/d = 0$ approach the one of a circular hole in an infinite plate except the range near $\psi = \pm 90°$ when $a/b \to 0$. Namely, the values of $\sigma_\theta/\sigma^\infty$ of problem A, B, C approach the ones of a circular hole under biaxial tension ($K_t = 2$), pure shear ($K_t = 4$), and uniaxial tension ($K_t = 3$), respectively.

Figs. 7–11 show stress distribution along the boundaries of problem C when $a/b = 2.0$, 1.0, 1/2, 1/4, 1/8 with $b/d = 0$, 1/3, 1/2, 2/3, 0.8, 0.9. Tsuchida's results (1976) of $a/b = 1.0$ coincide with the present results very well. As a result of comparison among Figs. 7–11, it is found that the position and magnitude of maximum stress varies depending on a/b and b/d. When a/b is close to unity, the interaction appears near the inside of two cavities as an increase of stress. On the other hand, as $a/b \to 0$ ($b \to \infty$), the interaction appears depending on the location of the boundary as an increase or decrease of stress, which is in a different way of the one of $a/b = 1$. The present method is found to yield the accurate value of σ_θ max, whose position varies slightly depending on a/b and b/d. If the interaction is small when $b/d \leqslant 1/2$, the variation of σ_θ is not very large (see Figs. 5,7–11). However, if $b/d \to 1$ and the interaction becomes larger, the variation of σ_θ becomes complicated especially for the extreme cases of $a/b \to 0$.

The magnitude and position of maximum stress of two ellipsoidal cavities are shown in Table 3 when $a/b = 2.0$, 1.0, 1/2, 1/4, 1/8, 1/50 with $b/d = 0$, 1/3, 1/2, 2/3, 0.8, 0.9. As shown in Table 3, the present results have good convergency to the fifth digit. In this analysis exact body force density to make a single
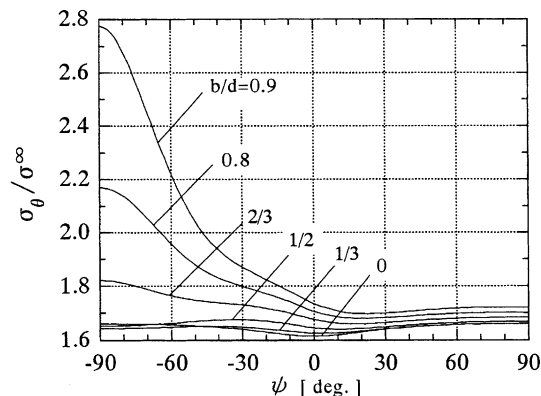

Fig. 7. Distribution of stress in Fig. 1(c) ($N = 2$, $a/b = 2.0$, $\theta = \pi/2$).
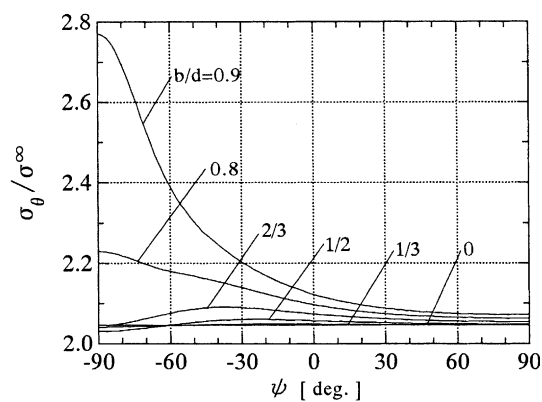
Fig. 8. Distribution of stress in Fig. 1(c) ($N = 2$, $a/b = 1.0$, $\theta = \pi/2$).
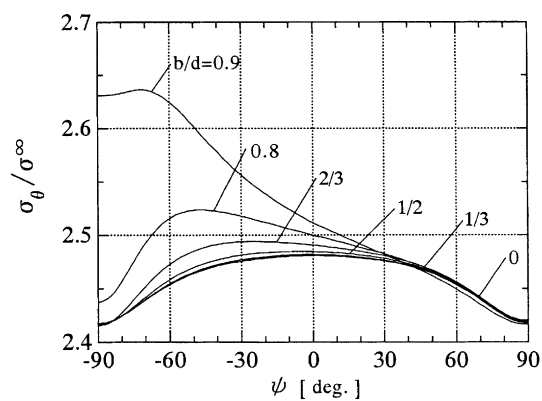

Fig. 9. Distribution of stress in Fig. 1(c) ($N = 2$, $a/b = 1/2$, $\theta = \pi/2$).
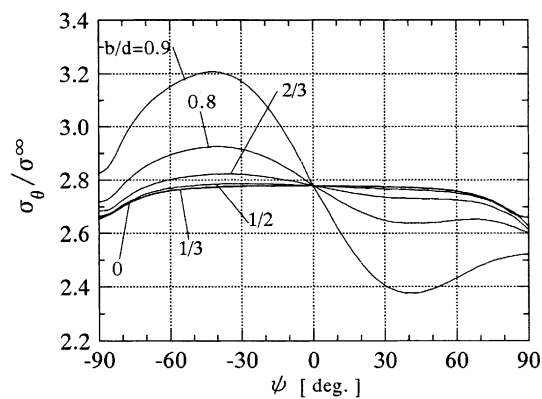

Fig. 10. Distribution of stress in Fig. 1(c) ($N = 2$, $a/b = 1/4$, $\theta = \pi/2$).
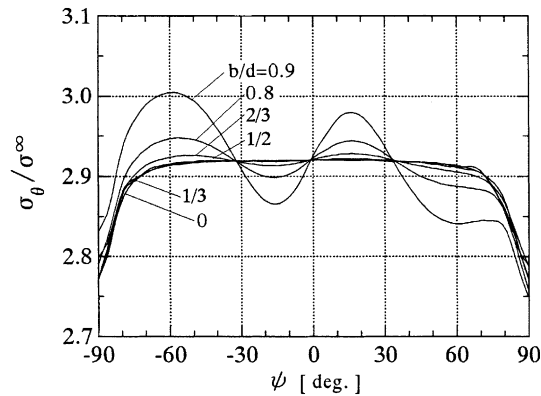
Fig. 11. Distribution of stress in Fig. 1(c) ($N = 2$, $a/b = 1/8$, $\theta = \pi/2$).

Table 3
Magnitude and position of the maximum stress of two ellipsoidal cavities in Fig. 1

b/d	a/b												
	2.0		1.0		1/2		1/4		1/8		1/50	
	(deg)	$K_{t\,max}$	(deg)	$K_{t\,max}$	(deg)	$K_{t\,max}$	(deg)	$K_{t\,max}$	(deg)	$K_{t\,max}$	(deg)	$K_{t\,max}$
0	±90	1.6601	−90 to 90	2.0455	0	2.4804	0	2.7772	0	2.9199	0	3.0226
1/3	90	1.6605	−14	2.0491	−1	2.4814	−13	2.7780	5	2.9202		−
1/2	−35	1.6747	−24	2.0598	−7	2.4844	−31	2.7859	12	2.9219		−
2/3	−90	1.8208	−37	2.0905	−24	2.4938	−37	2.8223	16	2.9281		−
0.8	−90	2.1705	−90	2.2295	−47	2.5240	−40	2.9255	−56	2.9477		−
0.9	−90	2.7754	−90	2.7724	−72	2.6363	−42	3.2074	−59	3.0044	−90	3.1218

ellipsoidal cavity of revolution is used. Therefore the method of analysis can be applied to the case for more extreme value of a/b and also to the case $b/d \rightarrow 1$.

5. Results and discussion for a row of ellipsoidal cavities

Table 4 shows convergence of the stresses at points A ($\psi = 90°$, $j = 1$) and B ($\psi = -90°$, $j = 1$), C ($\psi = 90°$, $j = 2$) of three spherical cavities in a body under biaxial, pure shear and uniaxial tension with increasing the collocation number M when $N = 3$, $a/b = 1.0$, $b/d = 0.9$, $\sigma^\infty = 1$, $v = 0.3$. The present results have good convergence to the fifth digits when $M = 24$. Table 5 shows the magnitude and position of the maximum stress, and the stresses at the points A, B, C of three spherical cavities in comparison with the results of Tsuchida et al. (1978) when $N = 3$, $a/b = 1.0$, $\sigma^\infty = 1$, $v = 0.3$ with $a/d = 0 \sim 0.9$. The present results and Tsuchida's results coincide with each other to the fourth significant digits in most cases.

Fig. 12 shows the relationship between $K_{t\,max}$ and $1/N^2$ when $a/b = 1.0$ with $b/d = 1/3$, 1/2, 2/3, 0.8, and Fig. 13 shows the one when $a/b = 1/4$ with $b/d = 1/3$, 1/2, 2/3, 0.8. Recently, Isida and Igawa (1994) have shown the linear relationship between $K_{t\,max}$ and $1/N$ for a row of elliptical holes (2D problem);

Table 4
Convergency of stresses at points *A* and *B*, *C* concentration factor $\sigma_\theta|_{\theta=\pi/2}/\sigma^\infty$ of three spherical cavities ($N = 3$, $a/b = 1.0$, $b/d = 0.9$, $v = 0.3$)

ψ (deg)	M	Biaxial	Pure shear	Uniaxial
j = 1				
−90	12	2.8300	2.7800	2.8050
	16	2.8300	2.7800	2.8050
	20	2.8300	2.7800	2.8050
	24	2.8300	2.7800	2.8050
90	12	2.2000	1.9500	2.0750
	16	2.2000	1.9500	2.0750
	20	2.2000	1.9500	2.0750
	24	2.2000	1.9500	2.0750
j = 2				
90	12	2.8400	2.7800	2.8100
	16	2.8400	2.7800	2.8100
	20	2.8400	2.7800	2.8100
	24	2.8400	2.7800	2.8100

Table 5
Stress concentration factors of three spherical cavities ($N = 3$, $a/b = 1.0$)

a/d	$j = 1$				$j = 2$		
	ψ (deg)	$K_{t\,max}$	K_{tA}	K_{tB}	ψ (deg)	$K_{t\,max}$	K_{tC}
0	−90 to 90 (−90 to 90)	2.0455 (2.045)	2.0455 (2.045)	2.0455 (2.045)	−90–90 (−90–90)	2.0455 (2.045)	2.0455 (2.045)
0.1	−10	2.0455	2.0455	2.0453	0	2.0455	2.0454
0.2	−10 (−10)	2.0463 (2.046)	2.0455 (2.045)	2.0446 (2.045)	0 (0)	2.0468 (2.047)	2.0447 (2.045)
0.3	−15	2.0486	2.0456	2.0425	0	2.0503	2.0428
0.4	−15 (−15)	2.0530 (2.053)	2.0453 (2.046)	2.0375 (2.038)	0 (0)	2.0571 (2.057)	2.0388 (2.039)
0.5	−23	2.0612	2.0484	2.0307	0	2.0687	2.0336
0.6	−31 (−30)	2.0769 (2.077)	2.0516 (2.052)	2.0308 (2.031)	±15 (±15)	2.0871 (2.087)	2.0361 (2.036)
0.7	−41	2.1067	2.0575	2.0702	±36	2.1188	2.0779
0.8	−90 (−90)	2.2413 (2.241)	2.0651 (2.065)	2.2413 (2.241)	±90 (±90)	2.2508 (2.251)	2.2508 (2.251)
0.9	−90	2.8050	2.0750	2.8050	±90	2.8100	2.8100

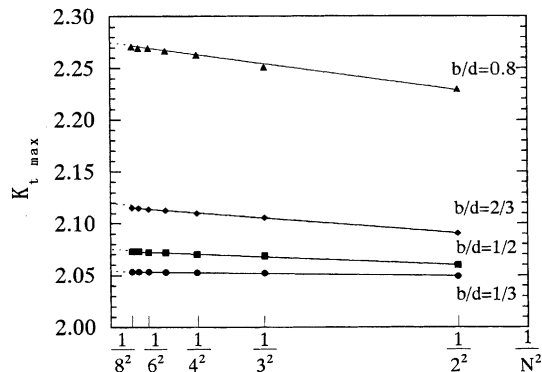Results of Tsuchida et al. (1978) in paranthesis.

Fig. 12. Relationship between $K_{t\,max}$ and $1/N^2$ in a row of elliptical cavities ($a/b = 1.0$, $\theta = \pi/2$).
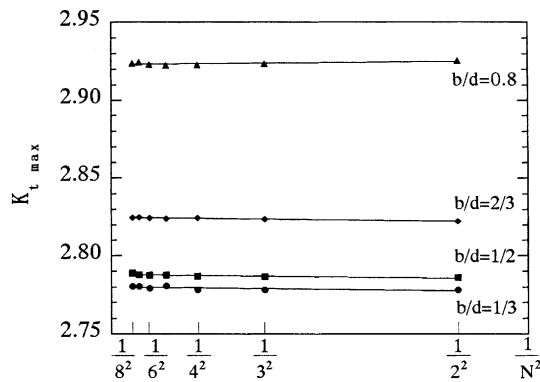
Fig. 13. Relationship between $K_{t\,max}$ and $1/N^2$ in a row of elliptical cavities ($a/b = 1/4$, $\theta = \pi/2$).

however, for a row of elliptical cavities (3D problem) we have a linear relationship between $K_{t\,max}$ and $1/N^2$. Those relationships are related to the fact that each cavity can be replaced by the distribution of self-equilibrating body forces. By using the linear relationship, the magnitudes and positions of the maximum stresses are shown in Table 6 when $N \to \infty$, $a/b = 2.0$, 1.0, $1/2$ and $1/4$ with $b/d = 0$, $1/3$, $1/2$, $2/3$, 0.8,

Table 6
Extrapolated stress concentration factors of an infinite row of elliptical cavities ($N \to \infty$)

a/b	b/d	Outermost cavity ($j = 1$)				Central cavity ($j = (N+1)/2$)		
		ψ (deg)	$K_{t\,max}$	K_{tA}	K_{tB}	ψ (deg)	$K_{t\,max}$	K_{tC}
2	0	±90	1.660	1.660	1.660	±90	1.660	1.660
	1/3	90	1.660	1.660	1.648	±35	1.652	1.643
	1/2	−30	1.679	1.673	1.656	±19	1.695	1.669
	2/3	−90	1.844	1.691	1.844	±90	1.885	1.885
	0.8	−90	2.235	1.717	2.235	±90	2.322	2.322
	0.9	−90	2.894	1.745	2.894	±90	3.037	3.037
1	0	−90 to 90	2.046	2.046	2.046	−90 to 90	2.046	2.046
	1/3	−10	2.050	2.048	2.043	0	2.053	2.042
	1/2	−25	2.062	2.048	2.032	0	2.073	2.035
	2/3	−35	2.096	2.056	2.052	±25	2.117	2.065
	0.8	−90	2.244	2.068	2.244	±90	2.273	2.273
	0.9	−90	2.812	2.079	2.812	±90	2.863	2.863
1/2	0	0	2.480	2.417	2.417	0	2.480	2.417
	1/3	−1	2.481	2.418	2.417	0	2.483	2.418
	1/2	−6	2.485	2.420	2.416	0	2.490	2.417
	2/3	−24	2.496	2.429	2.418	0	2.504	2.421
	0.8	−47	2.526	2.413	2.445	±44	2.533	2.449
	0.9	−73	2.646	2.423	2.641	±74	2.642	2.641
1/4	0	0	2.777	2.659	2.659	0	2.777	2.659
	1/3	−19	2.780	2.654	2.655	0	2.777	2.656
	1/2	−33	2.789	2.625	2.635	0	2.780	2.668
	2/3	−37	2.825	2.655	2.675	±10	2.784	2.659
	0.8	−43	2.925	2.616	2.651	±39	2.793	2.676
	0.9	−42	3.151	2.545	2.809	±62	2.819	2.714

0.9. In Table 6 the stresses at the points A, B ($\psi = \pm 90°$) on the outermost cavities ($j = 1$) and the stress at the point C ($\psi = +90°$) on the central cavities ($j = (N+1)/2$) are tabulated. In most cases in Table 6, the maximum stress occurs at the central cavity except for three case: (1) $a/b = 2.0$ and $b/d = 1/3$, (2) $a/b = 1/2$ and $b/d = 0.9$, (3) $a/b = 1/4$.

Fig. 14 shows stress distribution along the boundaries of ellipsoidal cavities $j = 1$, 2, 3 when $N = 5$, $a/b = 1.0$, $b/d = 0.8$, and Fig. 15 shows the one when $a/b = 1/4$, $b/d = 0.8$. Fig. 16 shows the magnitude and position of the maximum stress at each cavity with varying the number of cavities $N = 2$–8 when $a/b = 1.0$, $b/d = 0.8$, and Fig. 17 shows the one when $a/b = 1/4$, $b/d = 0.8$. From Figs. 14–17, it is found that the stress distributions along each cavity are similar to each other except for the one of the outermost cavity. The maximum stress is found to appear at the outermost or central cavity depending on a/b and b/d. Fig. 18 shows the stress distribution along the boundaries of the central and outermost ellipsoidal cavities when $a/b = 1.0$, $b/d = 2/3$ with varying the number of cavities N.
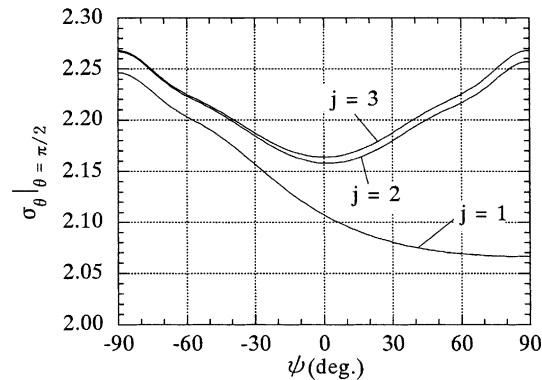

Fig. 14. Distribution of stress σ_θ in five spherical cavities ($N = 5$, $a/b = 1.0$, $b/d = 0.8$, $\theta = \pi/2$).
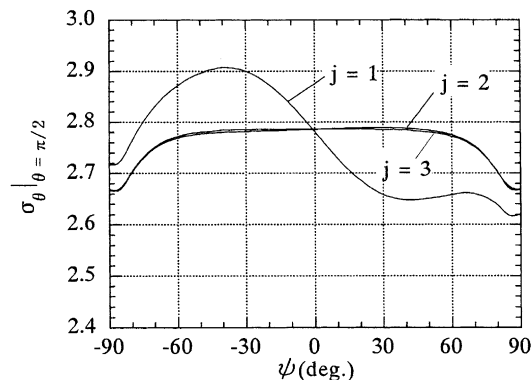

Fig. 15. Distribution of stress σ_θ in five elliptical cavities ($N = 5$, $a/b = 1/4$, $b/d = 0.8$, $\theta = \pi/2$).
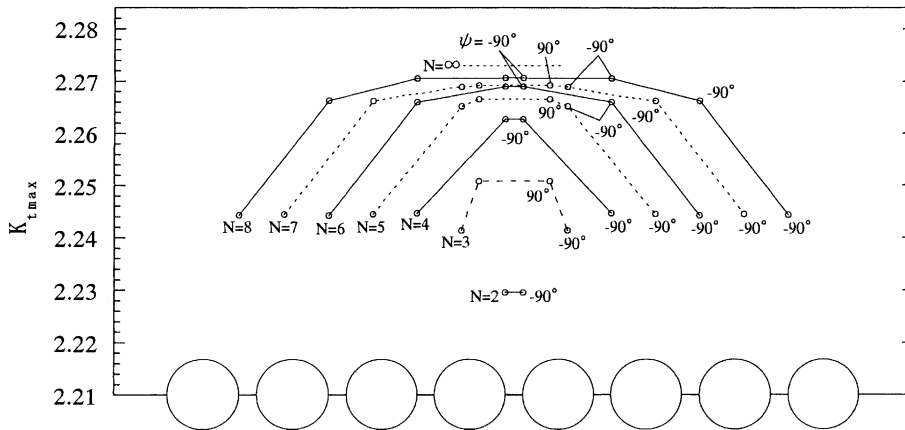
Fig. 16. Variation of $K_{t\,max}$ of infinite body containing a row of ellipsoidal cavities ($a/b = 1.0$, $b/d = 0.8$, $\theta = \pi/2$).
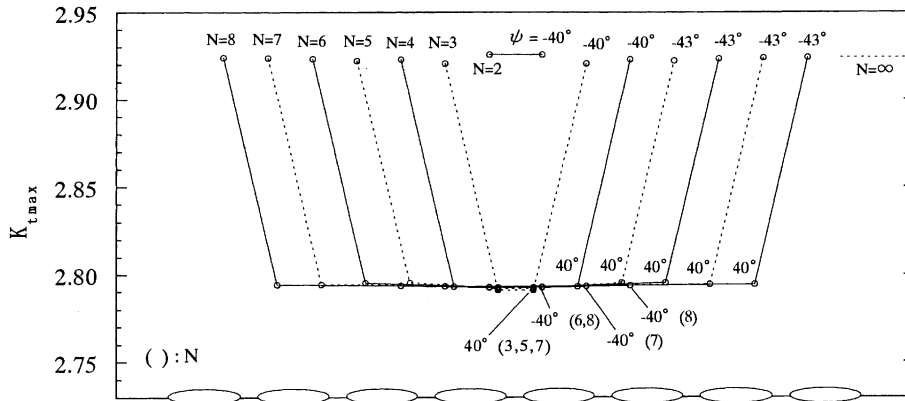

Fig. 17. Variation of $K_{t\,max}$ of infinite body containing a row of ellipsoidal cavities ($a/b = 1/4$, $b/d = 0.8$, $\theta = \pi/2$).
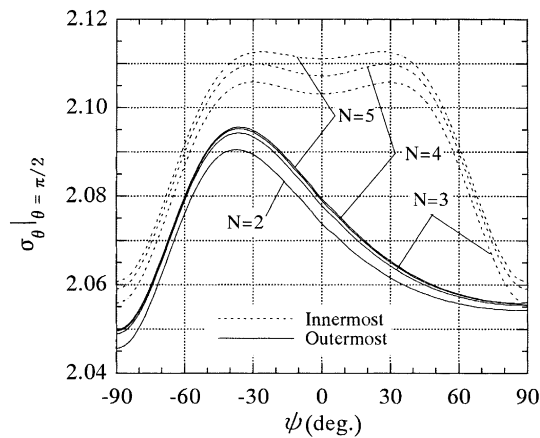

Fig. 18. Distribution of stress at the innermost and outermost cavity in a row of elliptical cavities ($a/b = 1.0$, $b/d = 2/3$, $\theta = \pi/2$).

6. Conclusion

In this study, by using a system of singular integral equations of the body force method, a row of revolutional ellipsoidal cavities in an infinite body under asymmetric uniaxial tension are considered. The conclusion can be made as follows:

(1) The problem is solved on the superposition of two auxiliary loads; (i) biaxial tension and (ii) plane state of pure shear. These problems are formulated as a system of singular integral equation with Cauchy-type singularities, where the densities of body forces distributed in the r, θ, z directions are unknown functions. In order to satisfy the boundary conditions along the ellipsoidal boundaries, eight kinds of fundamental density functions proposed in our previous paper are applied. The present method is found to give rapidly converging numerical results for stress distribution along the boundaries.
(2) For two and three spheroidal cavities, the results of the present analysis and the ones of Tsuchida et al. are in good agreement.
(3) For a row of elliptical cavities, it is found that the maximum stress concentration $K_{t\,\max}$ is nearly proportional to $1/N^2$, where N is the number of cavities. The maximum stress is found to appear at the outermost or central cavity depending on the shape and spacing of cavities.
(4) The magnitudes and positions of the maximum stresses are tabulated for various shape and distance of cavities for $N = 2$ and $N \to \infty$. The stress distribution along the boundaries are shown for various geometrical conditions.

References

Atsumi, A., 1960. Stresses in a circular cylinder having an infinite row of spherical cavities under tension. J. Appl. Mech., Trans. ASME, Ser. E 27 (1), 87–92.
Eubanks, R.A., 1965. Stress interference in three-dimensional torsion. J. Appl. Mech., Trans. ASME, Ser. E 32 (1), 21–25.
Goree, J.G., Wilson, H.B., 1967. Axisymmetric torsional stresses in a solid containing two partially bonded rigid spherical inclusions. J. Appl. Mech., Trans. ASME, Ser. E 34 (2), 313–320.
Isida, M., Igawa, H., 1994. Some asymptotic behavior and formulae of stress intensity factors for collinear and parallel cracks under various loadings. Int. J. Fract. 65, 247–259.
Hill, J.L., 1966. Pure torsion of an infinite solid containing two rigid spherical inclusions. J. Appl. Mech., Trans. ASME Ser. E 33 (1), 201–203.
Miyamoto, H., 1957. On the problem of the theory of elasticity for a region containing more than two spherical cavities (First report: Theoretical calculations). Trans. Jpn. Soc. Mech. Engrs. (JSME) 23, 431–436 (in Japanese).
Murakami, Y., Noda, N.-A., Nisitani, H., 1986a. Application of body force method to the analysis of stress concentration of an axisymmetric body under bending: I. Basic theory and application to several simple problems. Int. J. Solids Struct. 22, 23–37.
Murakami, Y., Noda, N.-A., Nisitani, H., 1986b. Application of body force method to the analysis of stress concentration of an axisymmetric body under bending: II. Stress concentration of a cylindrical bar with a semi-elliptical circumferential notch under bending. Int. J. Solids Struct. 22, 39–53.
Nisitani, H., 1963. On the tension of an elastic body having an infinite row of spheroidal cavities. Trans. Jpn. Soc. Mech. Engrs. (JSME) 29, 765–768.
Nisitani, H., 1967. The two-dimensional stress problem solved using an electric digital comiuter. J. Jpn. Soc. Mech. Eng. 70, 627–632, Bull. Jpn. Soc. Mech. Engrs. 11 (1968) 14–23.
Nisitani, H., Noda, N.-A., 1984. Stress concentration of a cylindrical bar with a v-shaped circumferential groove under torsion, tension or bending. Engrg. Fract. Mech. 20, 743–766.
Noda, N.-A., Matsuo, T., 1993. Numerical solution of singular integral equations of the body force method in notch problems (Second report: Analysis of interaction problems of notches under general loading conditions). Trans. Jpn. Soc. Mech. Engrs. (JSME) 59, 1964–1970 (in Japanese).
Noda, N.-A., Matsuo, T., 1995a. In: Erdogan, F., (Ed.), Singular Integral Equation Method in the Analysis of Interaction between Cracks and Defects, ASTM STP 1220.
Noda, N.-A., Matsuo, T., 1995b. Singular integral equation method in optimization of stress-relieving hole: a new approach based on the body force method. Int. J. Fract. 70, 147–165.

Noda, N.-A., Matsuo, T., 1996. Singular integral equation method in stress concentration problem. Int. J. Solid Struct. 34, 2429–2444.

Noda, N.-A., 1984. Stress Concentration Problem of a Cylindrical Bar with V-Shaped Circumferential Groove under Torsion, Tension and Bending, Ph.D. dissertation, Kyusyu University, 1984.

Noguchi, H., Nisitani, H., Goto, H., Mori, K., 1987. Semi-infinite body with a semi-ellipsoidal pit under tension. Trans. Jpn. Soc. Mech. Engrs. (JSME) 53, 820–826 (in Japanese) [JSME Int. J. Series I 32(1) (1989) 14–22].

Shelly, J.F., Yu, Y.-Y., 1966. The Effect of two rigid spherical inclusions on the stresses in an infinite elastic solid. J. Appl. Mech., Trans. ASME, Series E 33 (1), 68–74.

Sternberg, E., Sadowsky, M.A., 1952. On the axisymmetric problem of the theory of elasticity for an infinite region containing two spherical cavities. J. Appl. Mech., Trans. ASME 19, 410.

Tsuchida, E., Nakahara, I., Kodama, M., 1976. Asymmetric problem of elastic body containing several spherical cavities (First report: Two spherical cavities in an elastic body). Trans. Jpn. Soc. Mech. Engrs. (JSME) 42, 46–54 (in Japanese).

Tsuchida, E., Nakahara, I., Kodama, M., 1978. Asymmetric problem of elastic body containing several spherical cavities (Second report: Three spherical cavities in an elastic body). Trans. Jpn. Soc. Mech. Engrs. (JSME) 44, 1876–1883 (in Japanese).